Volumetric Modeling of Colored Pencil Drawing

Saeko Takagi Issei Fujishiro† Masayuki Nakajima

Department of Computer Science
Tokyo Institute of Technology
2-12-1, O-okayama, Meguro-ku,
Tokyo 152-8552, Japan

†Department of Information Sciences
Ochanomizu University
2-1-1, Otsuka, Bunkyo-ku,
Tokyo 112-8610, Japan

Abstract

Not only photorealistic rendering but non-photorealistic rendering is considered an important research topic in artistic image synthesis. However, little attention has been given to colored pencil drawing. This paper proposes a volume graphics model for colored pencil drawing. The model consists of three sub-models, which describe in a volumetric fashion, the microstructure of paper, pigment distribution on paper, and pigment redistribution, respectively. The model takes advantage of volumetric offset distance accessibility and line integral convolution, and thus is highly controllable with a small number of parameters. A couple of synthesized color pencil drawing data sets are rendered using an existing volume visualizer to empirically prove that the model is descriptive enough to produce realistic images of colored pencil drawing.

1. Introduction

In recent years, computer graphics(CG) has been utilized through various mass media and diffused extensively. Although photorealistic rendering is used to create most of these images, various types of non-photorealistic rendering, such as pen-and-ink, oil and watercolor painting, are considered important research topics.

Among these topics, we have focused on *colored pencil drawing*(*CPD*). Formerly CPD was used as a means of study or for preliminary sketches to be developed further in paintings or sculpture. Hence, CPD was regarded as secondary in relation to the painted or finished work. However, CPD has recently become an artform in its own right. In particular, CPD is often being used for package illustration and picture books. In its current state, CPD deserves to be a very viable research topic.

One of the salient features of CPD is a gentle appearance for human eyes because of the soft, harsh, and almost misty representation, as shown in Figure 1. CPD-like images could be emulated on screen by combining several functions provided by existing digital paint systems. At present, however, there exists no system that directly supports the CPD appearance and techniques. There are quite a number of CPD techniques[6, 9], and faithful reproduction of these is essential in order to capture the charm of CPD.

We first started this research with identification of the general production process of an actual CPD, and established two-dimensional(2D) sub-models for pigment distribution and redistribution. Although acceptable results were obtained using our pigment redistribution sub-model[12], it turned out that it is very difficult for the 2D pigment distribution sub-model to represent the tints of real CPD. The sub-model only generated results similar to crayon drawings, which can be produced easily with a pencil function provided by current digital painting systems (Figure 2). As the 2D pigment distribution sub-model did not produce desirable results, we focused on the usage of the redistribution sub-model to modify actual CPD images taken with a scanner. In this case, we found another problem that the movement of pigments was too uniform and smooth, even after perturbation factors were added to the governing algorithm.

Drawing paper has a natural *texture* which can be recognized even by the naked eye. We considered that a CPD-like appearance would not be obtained until a model was constructed accounting for the paper's fine structure. In order to address the issue, we have turned our eyes to a three-dimensional(3D) approach to describe the interaction between the texture of paper and the pencil lead or brush.

Guo's Indian ink painting[5] and Curtis' watercolor[4] consider the 3D minute structure of painting materials. Both pay attention to the capillary movement of water on paper, that is, the relation between paper and water, rather than the relation between paper and pigments. These models of water movement could be used for CPD only when the colored pencil was water-soluble and a large amount of water was added. However, such a case is not usual.

Learning from our initial attempts, we have constructed a CPD model which considers the 3D structure of draw-

Figure 1. Example of an actual colored pencil drawing.

Figure 2. Example of an image drawn with *Painter*, an existing painting tool.

ing materials[13, 14]. The model is based on the observation and investigation of real CPDs. It consists of three sub-models, which describe in a volumetric fashion, the microstructure of paper, pigment distribution on paper, and pigment redistribution, respectively. The paper-microstructure sub-model describes the microstructure of paper using a few geometric primitives corresponding to the components which are thought to have major influence on paper texture. The resulting data is then 3D scan converted into a paper volume[8]. On the converted volumetric data, pigment distribution and redistribution are evaluated to yield the natural appearance of colored pencil strokes. In addition to the stroke direction and the degree of pigment-acceptance depending on ingredients of paper components, the pigment distribution sub-model makes use of volumetric offset distance accessibility[10] in order to locate the area which the tip of the lead can reach. The accessibility is also used in two types of pigment redistribution sub-models, specifically running a wet brush over a CPD-surface and eraser effects. In the former redistribution sub-model, the movement of pigments by means of a wet brush is represented with a 3D extended line integral convolution[3].

Figure 3. Electron microscope photograph of drawing paper processed with chemicals.

The voxels which contribute to the convolution are identified, and the contribution weight for each of the voxels is determined by the distance to the target voxel. The use of these two algorithms makes the present model highly controllable.

It should be noticed here that *volume* is adopted as the common data structure for the sub-models. *Volume graphics* has emerged as a CG research sub-field and has the potential to surpass the traditional surface graphics in representation, operation, and rendering of 3D objects[8]. Relying on volumetric representation is a unique approach to sophisticated image synthesis for the application of digital painting.

The rest of this paper is organized as follows. In the next section, the 3D microstructure of actual CPDs is briefly overviewed. Section 3 describes our CPD model. In Section 4, each step of the image synthesis process is delineated with the rendering of sample CPD volumes, to empirically prove the feasibility of our model. Finally, Section 5 concludes the paper and outlines several ideas for future work.

2. Microstructure of actual colored pencil drawing

2.1. Drawing paper

For the purpose of modeling, we investigated the structure of actual paper and the conditions of real CPDs. The paper most generally used in CPD is a drawing paper, which is a slightly rough, non-coated paper[7]. The magnified view of the paper surface is shown in Figure 3 [1], where the black areas correspond to pulp fiber and the white areas to loading matter. The loading matter has talc or kaolin as its main ingredients, and is mixed with the pulp to improve smoothness, ink-acceptance, and paper opacity[7]. It occupies 10-20% of the total weight of paper. Although a very small amount of chemicals for the reduction of blotting is added, the remainder is almost pulp. Therefore, the drawing paper is considered as a combination of pulp, loading matter, and air.

[1] Courtesy of Nippon Paper Industries Co., Ltd.

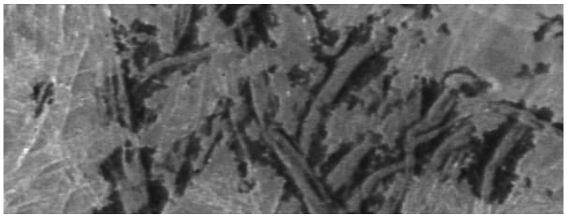

(a) After basic drawing.

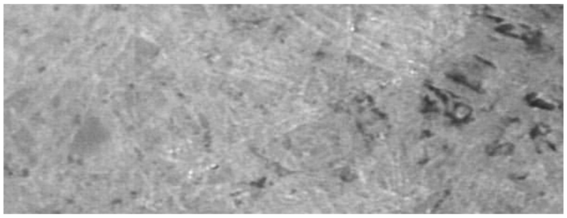

(b) After creating a wash.

Figure 4. Magnified images of a colored pencil drawing by digital microscope (lens magnification: 500×).

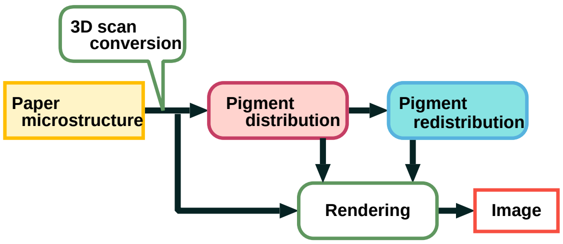

Figure 5. Relationships among sub-models.

2.2. Colored pencil drawings

Figure 4 shows a real CPD observed through a digital microscope. In Figure 4 (a), the areas colored dark indicate plateaus, on which we observe finer irregularities, which easily peel off pigment from a lead. Under the influence of the loading matter with a high ink-acceptance and the bonding agent in the lead, pigment tends to adhere to the areas covered with loading matter and pigment.

When using water-soluble colored pencils, *watering* is a CPD technique for redistributing pigment with a wet brush. After running a wet brush over a CPD-surface such as shown in Figure 4 (a), pigment is spread and blended with water. The effect is shown in Figure 4 (b). However, even after watering, all of the pigments do not necessarily dissolve in water. The quality of the bonding agent, the quantity of water, the thickness of pigments, and brush pressure are the main factors that affect the degree of pigment dissolution. In addition, since a pigment-lump is comparatively large even if it dissolves, the transport of pigments is governed not only by capillary motion but also by the movement of the brush. This is an obvious characteristic of CPD, which differentiates it from other types of drawings, leading to the governing mechanism for our 3D CPD model, as described in the next section.

3. Colored pencil drawing model

3.1. Model structure

Figure 5 shows the relationships among the CPD submodels proposed in this paper.

First, drawing paper is modeled geometrically using several 3D primitives. The modeled paper is then 3D scan converted into a volumetric form, in which the composition elements are discretely distinguishable.

The pigment distribution and the pigment redistribution sub-models are constructed as operational models that operate upon the paper volume data. The two sub-models reflect the paper microstructure, and take into account the hardness or softness of a lead.

For the purpose of optically faithful rendering, we used an existing volume visualizer, *VolVis* [2] [1], known for supporting volumetric ray tracing[11].

3.2. Preliminaries

In the field of chemistry, the concept of accessibility was introduced in the 1970's for modeling a boundary where solvent molecules come into contact with a set of solute molecules. More recently, G. Miller imported the concept into the field of computer graphics[10]. By assuming the brush tip to be approximated by a spherical probe and specifying the radius of a probe which is able to reach between objects, he defined two kinds of accessibility to locate dirty area covered with dust unremovable by brush cleaning. We chose to use one of these specific types of accessibility, called *offset distance accessibility*(*ODA*). In our work, the point of a pencil and the tip of a brush are assumed to be a sphere, and the *volumetric* ODA is used for calculating the roughness of paper (Sections 3.4 and 3.5). Because the ODA was originally defined for solids, we have to perform a binary classification on voxels of the CPD-volume according to the density of composition materials with respect to prefixed thresholds.

The original *line integral convolution*(*LIC*)[3] is a type of filtering which transforms a pixel value into a weighted average of the pixel values along the local streamline obtained through a vector field. The set of pixels involved in

[2] VolVis is freeware developed and distributed by the Visual Computing Center, the State University of New York at Stony Brook.

the calculation is referred to as the *kernel*. An LIC-filtered image looks smeared along the given vector field. LIC has been used mainly in scientific visualization. In this paper, LIC is extended to 3D by adding height information to the 2D data, and then adopted to approximate the movement of pigments in the pigment redistribution sub-model (Section 3.5). A stroke vector is used instead of a local streamline in the extended LIC. Pigment redistribution corresponding to the pencil pigment characteristics and the brush stroke speed can be simulated using the LIC by adjusting the length of the convolution kernel, estimating the location of the voxels which contribute to the LIC calculation, and finding the contribution of the convolution kernel. The approach to identifying effective voxels in this paper is an original extension to LIC.

3.3. Paper microstructure

When modeling the paper microstructure, the composition elements are limited to those needed in expressing the appearance of drawing paper. As mentioned in Section 2.2, drawing paper is mostly composed of pulp, loading matter, and air. In our model, these elements are modeled geometrically using a modified primitive instancing.

A pulp primitive is represented initially by a cylinder. Then, reflecting the manufacturing process, the cylinder primitives are randomly constricted, defaced, and sparsely fringed as shown in Figure 6 (a). To generate a fiber net, pulp primitives with varied parameters are placed globally with a unique orientation, but locally with random orientations. When generating the fiber net, interference among pulp primitives is disregarded, spontaneously leading to an intertwined pulp net with varying density. Unlike in the ordinary primitive instancing, ignoring primitive interference is rather necessary for generating the pulp net.

We chose to represent a loading matter primitive by a thick disk, because talc, which is its principal ingredient, forms flat crystals. In a piece of real paper, loading matter hardens into various sizes. In order to represent this phenomenon, the radius, thickness, and material density of the

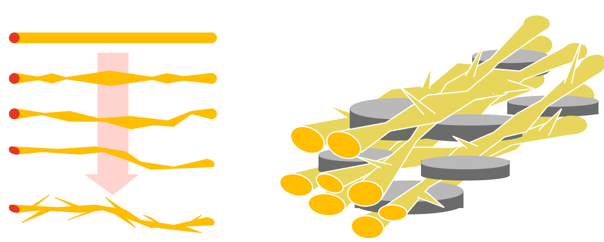

Figure 6. (a) Progressive refinement of a pulp primitive. (b) Geometrical data of paper.

disk primitives is varied.

As shown in Figure 6 (b), The disks are placed at random locations using the following set operation:

$$(L - P) \cup P, \quad P : pulp,\ L : loading\ matter,$$

where a gap is likely to accept loading matter, and pulp remains the same as before. Again, we ignore the intersection among loading matter primitives. If intersection occurs, the new primitive is simply added to existing loading matter. Therefore, even if the density of the primitives is given constant, the loading matter density appears to be distributed non-uniformly. In this way, paper data obtained from our sub-model is capable of reflecting the structure of real paper, in that the loading matter does not disturb the direction of the pulp, and the primitives are distributed in various shapes and densities. Moreover, by using talc disks with a varying density distribution, the model can generate more complex data.

Because the series of these models assumes the volume to be the common data representation, as described in Figure 5, the geometric data of paper should be 3D scan converted to generate the volumetric data (see Figure 7 (a)). Each voxel field value is a scalar which indicates the density of paper components or pigments at that coordinate. Then, our two drawing sub-models (Sections 3.4 and 3.5) are used to create a CPD on the paper volume.

3.4. Pigment distribution

Here a pigment distribution sub-model is proposed, which takes into account the paper microstructure. A colored pencil stroke is assumed to be a straight line segment with a constant width, and specified with the coordinates of the starting point, the direction vector on the (x, y) plane, and the width.

There are two ways in which pigment is distributed onto the surface of paper (Figure 7 (b)):

1. Pigments are shaved off from a lead by friction and deposited on a convex part of the paper.

2. Pigments adhere to the surface of paper, when a lead runs through areas covered with loading matter and pigments.

First, in both cases, ODA is used to identify which voxels are accessible. The radius of the probe which indicates the size of the lead edge is determined from the width of the stroke, and then the ODA value of the CPD volume is calculated. The ODA field is given in the form of a 2D horizontal array. We will now explain how to model the two types of distribution in more detail.

In the first phenomenon, a convex voxel along the pencil stroke direction peels off pigment from the lead, and the pigment distribution is performed as follows. The current

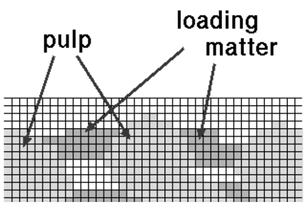

(a) Paper.

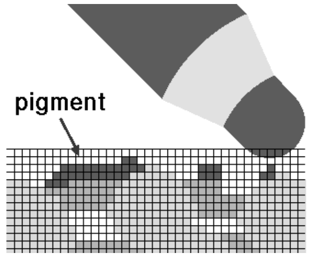

(b) Drawing.

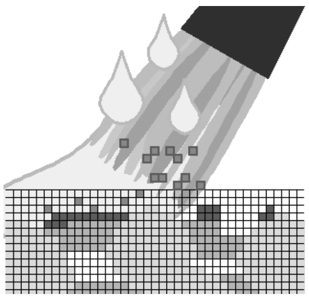
(c) Watering.

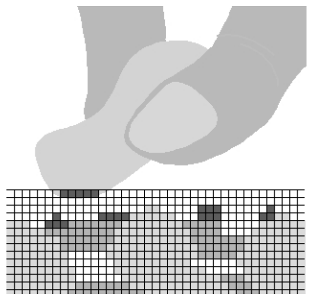
(d) Eraser effects.

Figure 7. Volumetric diagram of paper volume, pigment distribution, and redistribution concept in cross section.

voxel (x, y, z) in the stroke region is interpreted as a point (x, y) with height field value z. Given the stroke vector $\vec{v}$, if the ODA value of the current voxel is equal to 0, and the ODA values of the voxels located in the direction of $-\vec{v}$ from the current voxel are not equal to 0, then the current voxel (x, y, z) is judged to be convex along the pencil stroke direction. In other words, if a voxel becomes accessible following inaccessible voxel(s) against the stroke vector, the current voxel is considered to be a convex voxel against the pencil stroke direction, and it peels off pigment from the lead. The pigments peeled off by the convex voxel are scattered not on the current voxel but on some voxels located mainly in the direction of $-\vec{v}$ from the current voxel. The scattered pigments are fixed by means of two operators, which will be described at the end of this section.

For the second type of distribution, since loading matter and pigment have a high ink-acceptance, pigments tend to adhere to these voxels if they are accessible. By considering the fact that the lead is not only touched by voxels but also dragged across them, the lead voxels need to be accessible consecutively. If the ODA values of the consecutive voxels are equal to 0 in the stroke direction and these voxels contain pigment or loading matter, pigments are judged to adhere to the these voxels. The thickness of the pigments which adhere is determined from the density of the loading matter, the quality of the bonding agent contained in the lead, and

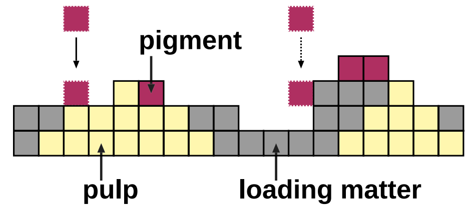

Figure 8. Two types of fixing operators, dropping pigments on top of materials (left), and attaching pigments to both the top and sides of loading matter or other pigments (right).

the stroke pressure. Using the thickness information, pigments are deposited on the target voxels.

Two types of fixing operators are used for depositing, where the distributed pigments adhere to the paper. One operator drops pigments on top of materials, and the other type attaches pigments to both the top and sides of loading matter or other pigments (Figure 8). These operators are designed on the basis of the fractal surface growth models [2].

3.5. Pigment redistribution

Learning from the observations and investigations of Section 2, and the initial attempts with the 2D model[12], we developed a pigment redistribution sub-model, which takes into account the microstructure of paper and pigments. In this paper, we propose two types of pigment redistribution sub-models for common CPD techniques: watering and eraser effects (Figure 7 (c) and (d)).

3.5.1. Watering

A flat brush with parameters for width and thickness is assumed for the redistribution. The coordinates of the starting point and the stroke vector on the horizontal plane are also given.

First, in the same way as in the pigment distribution sub-model, voxels accessible to a brush are identified with ODA. In this case, the probe radius is decided from the thickness of the brush. We assume that a pigment dissolves in water when a wet brush touches the pigment voxel. If a pigment voxel in the stroke region is accessible, the voxel has the possibility of dissolving. For these voxels, the degree of possibility is determined from the quantity of water contained in the brush, the quality of the bonding agent contained in the lead, and the stroke pressure. When the degree exceeds a pre-specified threshold, the voxel is emptied, that is, it becomes a *source voxel*.

In addition, a voxel can also begin to be emptied if it touches a source voxel in the vertical direction, depending

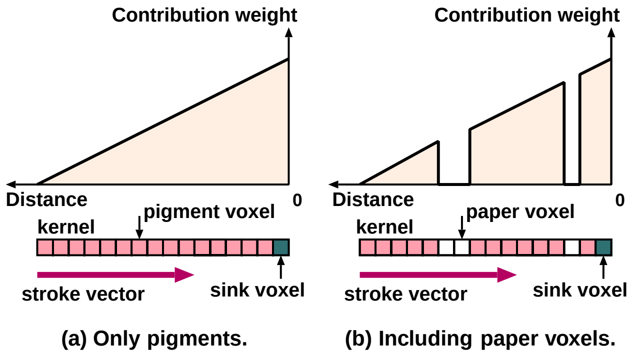

Figure 9. Weights assigned to voxels on a kernel.

Table 1. Composition elements of paper volumes in Figure 11.

	No.	1	2	3
pulp	radius	4	4	30
	length	400	500	600
	number	40,000	25,000	20,000
	volume(%)	81.106	70.500	67.994
talc	radius	20	30	40
	thickness	6	6	6
	number	20,054	14,582	12,006
	volume(%)	18.221	29.343	31.994

on the bonding agent in the lead. Whether or not the voxel actually begins to dissolve is also decided by the above-mentioned method.

After the source voxels are located, the brush stroke vector is used as a streamline for the LIC, and the pigment movements are calculated. A convolution kernel is defined on the height field. Its length is decided according to the quantity of water and the stroke speed. The source voxels in the convolution kernel also contribute to the calculation of the LIC. Non-pigment voxels, however, should not contribute to the calculation. Therefore we modified the kernel weights so that non-pigment voxels are skipped.

The contribution weight of a source voxel is decided from the distance between the voxel to the *sink voxel* in which the dissolved pigments collect (see Figure 9 (a)). Pigments removed with the brush can be expressed by setting the total sum of contribution weights from a source voxel to all surrounding voxels to be less than 1. If there are one or more non-pigment voxels on the kernel, as in Figure 9 (b), the convolution kernel is “worm-eaten.” If attention is paid not to how much influence a voxel receives from other voxels, but to how much contribution a voxel gives to other voxels, the intention of this contribution weight setting can be more easily understood.

Because some sink voxels fall outside of the stroke region at the end of the stroke, the pigments may vanish without any contribution. These vanishing pigments can be considered to be removed by the brush, reflecting the actual phenomenon.

The pigments calculated with the method are attached by a fixing operator in which pigments fall until reaching a paper voxel (see Section 3.4).

Because the probe radius, the kernel length, and the convolution weight of the LIC can abstract the quantity of water, the brush pressure, and the stroke speed, our model can easily reproduce various watering effects, such as blurring, and mixing colors.

3.5.2. Eraser effects

There are really many CPD eraser techniques, including correction, creating a soft tint or highlight, burnishing, and blending colors. Here, we will focus on reproducing the soft tint effect, because this technique has no substitute and is therefore imperative for creating CPDs with a soft impression.

A soft tint is obtained by applying light eraser strokes to CPD surfaces. The shape of the patted area with an eraser stroke is assumed to be ellipse. The involved parameters include the coordinates of the patting point, and the size and orientation of the ellipse. Additional key parameters are the softness of the eraser and the pressure of the eraser stroke.

Here again, ODA is referred to in order to evaluate which voxels are accessible to the eraser. The probe radius is decided from the softness of the eraser and the pressure of the eraser stroke. Here, an eraser is limited to move only in the vertical direction. The top few layers of accessible pigment voxels are emptied by an eraser stroke. The thickness of the emptied layers is estimated according to the softness of the eraser and the pressure of the eraser stroke.

4. Results

Our code has been implemented and performed on an SGI O2 system (CPU: R5000, Clock: 180MHz, RAM: 256MB). As mentioned above, we have used VolVis ver. 2.1 for volumetric rendering.

First, several paper volumes were generated based on our paper sub-model, then rendered (Figure 11 (a), (b), and (c)). The common size of the volumes is $2{,}048 \times 1{,}536 \times 6$ voxels, in each of which contains the primitives shown in Table 1.

Next, using the pigment distribution sub-model, we drew a *Pumpkin* on these paper volumes and rendered the resulting volumes, shown as Figure 11 (d), (e), and (f). As some pigment layers are added over the paper layer, the volume’s

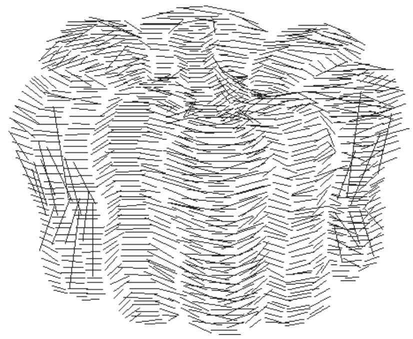

Figure 10. Strokes for *Pumpkin* in Figure 11.

size is changed to 2,480×1,536×10 voxels, to which the basic stroke sets (304 red strokes, 340 orange strokes, 325 yellow strokes, 143 brown strokes) are drawn with a width of 8. Figure 10 shows the sum total of strokes in wireframe. By evaluating the model which uses the accessibility to capture the paper microstructure, the scratchy strokes peculiar to CPDs are represented and the gentle appearance of CPD is reproduced. In addition, the same vestige of paper texture in scratched portions as in Figure 1 is very useful for increasing the naturalness of CPD.

Figure 12 (a) shows the case of drawing on brown paper. This image is rendered from the volume in Figure 11 (e). By the control of optic transfer functions, we can produce a different texture of paper from the same volume data set. This is an advantage of taking the volumetric approach from the viewpoint of interactivity.

Figure 12 (b) shows the watering effect applied to the CPD volume in Figure 11 (e). The volume size is again slightly increased to 2,480×1,536×12 voxels. On red and brown areas, 52 strokes of wet brush were drawn (the probe radius = 2, the basic kernel length = 60, and the stroke width = 30). It is observed that pigments which adhere due to the roughness of the pulp extend somewhat. Actually, the density distribution among pigment voxels is equalized, leading to pigment-lumps being spread thinly. The plausibility of our model is visually verified by comparison with the image in Figure 12 (c), which is an actual CPD after watering. The image in Figure 12 (b) is seen to faithfully reproduce the actual image.

Figure 13 shows another example of paper which is assumed to be the Japanese paper called "washi." The paper volume is the same as the one shown in Figure 11 (b), but the rendering parameter values are different. The CPD shown in Figure 14 (a) was drawn with 2,403 pencil strokes of width 6. Then, the two types of the redistribution sub-models ware evaluated. Watering with 98 brush strokes of width 15 ware given. The LIC kernel has 60 voxels in length, and the probe radius is equal to 2 (Figure 14 (b)). An eraser effect was added around the tip of the plant's leaf with the probe radius 8 (Figure 14 (c)). For comparison with these images, Figure 14 (d), (e), and (f) are real CPDs which were drawn in a similar manner. The stroke gets somewhat scratchy, expressing a light feeling which might be similar to real CPDs.

The timings to compose the paper volumes 1 and 2 are about 6 minutes, and about 18 minutes is needed for constructing the paper volume 3. If the ODA value is prespecified, which seems to need some ingenious contrivance, the pigment distribution and redistribution sub-models can be computed at an interactive rate. The image size is 800×600 pixels in all the resulting images. The rendering time is about 9-10 minutes in Figures 11 and 12 (except (c)), and about 10-11 minutes in Figures 13 and 14 (a), (b),and (c). Inherently, the rendering time for volume rendering is almost independent of the difference in influence of added effects.

5. Conclusions

On the basis of the preliminary research, we proposed a volumetric model for CPD. The model consists of three submodels describing paper microstructure, pigment distribution, and pigment redistribution. In the paper microstructure sub-model, using a modified method of primitive instancing, paper volume data is represented geometrically, followed by 3D scan conversion into a corresponding paper volume. In the pigment distribution sub-model, the profile of the paper structure along the pencil stroke direction can be estimated with ODA, and referred to for the decision of the pigment distribution extent. The paper materials were also considered in the sub-model. In the two types of pigment redistribution sub-models, ODA is also used. In addition, in the watering model, the movement of pigment is simulated by an innovative extension to LIC. To evaluate the entire model, the data representing several kinds of drawings are rendered by an existing volume visualizer. The resulting images show qualitative agreement with actual CPDs.

For further system development, we are currently interested in representing several remaining techniques in a volumetric fashion, and developing an original volume renderer specifically for CPDs. In the renderer, we plan to include the following items: definition of a convenient data format for CPD, color generation based on Kubelka-Munk theory, and support for subsurface scattering.

Acknowledgment

This work was financially supported in part by the Research Fellowships of the Japan Society for the Promotion of Science for Young Scientists. The authors appreciate valuable comments on the English from Karen Vierow of Nuclear Power Engineering Corporation.

(a) Paper volume 1. **(b) Paper volume 2.** **(c) Paper volume 3.**

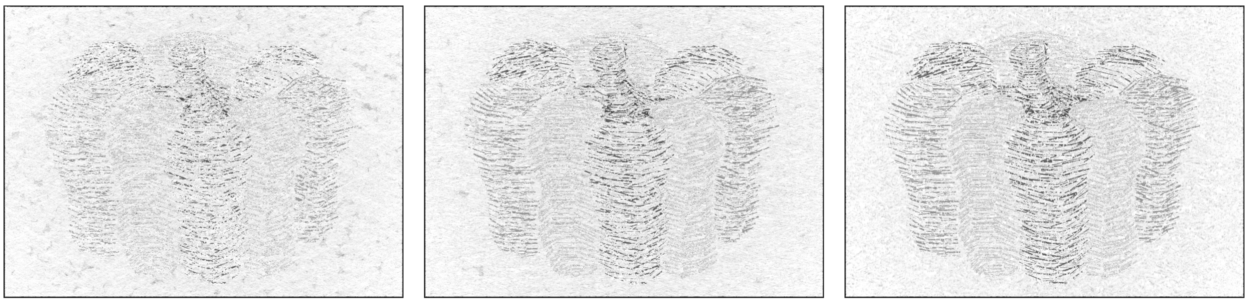

(d) CPD volume 1. **(e) CPD volume 2.** **(f) CPD volume 3.**

Figure 11. *Pumpkin* s on paper with different textures.

References

[1] R. Avila, T. He, L. Hong, A. Kaufman, H. Pfister, C. Silva, L. Sobierajski, and S. Wang. Volvis: A diversified volume visualization system. In *Proc. IEEE Visualization'94*, pages 31–38, October 1994.

[2] A. L. Barabasi and H. E. Stanley. *Fractal Concepts in Surface Growth*. Cambridge University Press, June 1995.

[3] B. Cabral and L. C. Leedom. Imaging vector fields using line integral convolution. In *Proc. ACM SIGGRAPH 93 (COMPUTER GRAPHICS Annual Conference Series)*, pages 263–272, August 1993.

[4] C. J. Curtis, S. E. Anderson, J. E. Seims, K. W. Fleischer, and D. H. Salesin. Computer-generated watercolor. In *Proc. ACM SIGGRAPH 97 (COMPUTER GRAPHICS Annual Conference Series)*, pages 421–430, August 1997.

[5] Q. Guo and T. L. Kunii. Modeling diffuse painting of sumie. In *Proc. IFIP WG 5.10 Working Conference*, pages 329–338, May 1991.

[6] I. Hutton-Jamieson. *Colored Pencil Drawing Techniques*. North Light Books, September 1986.

[7] T. Kadoya, Y. Sumi, and I. Yoshino. *Paper Science*. Chugai Sangyo Chosakai, June 1989.

[8] A. Kaufman, D. Cohen, and R. Yagel. Volume graphics. *IEEE Computer*, 26(7):51–64, July 1993.

[9] J. Martin. *The Encyclopedia of Colored Pencil Techniques*. Running Press, April 1997.

[10] G. Miller. Efficient algorithms for local and global accessibility shading. In *Proc. ACM SIGGRAPH 94 (COMPUTER GRAPHICS Annual Conference Series)*, pages 319–326, July 1994.

Figure 13. Japanese paper called "washi."

[11] L. W. Sobierajski and A. E. Kaufman. Volumetric ray tracing. In *Proc. ACM Volume Visualization Symposium'94*, pages 11–18, October 1994.

[12] S. Takagi and I. Fujishiro. Modeling of pigment spreading and blending with water in water-soluble colored pencil drawings. In *IPSJ SIG Notes, 96–CG–80*, pages 25–32, May 1996.

[13] S. Takagi and I. Fujishiro. Microscopic structural modeling of colored pencil drawings. In *ACM SIGGRAPH 97 The Art and Interdisciplinary Programs (Technical Sketches)*, page 187, August 1997.

[14] S. Takagi, I. Fujishiro, and M. Nakajima. Volume graphics modeling of colored pencil drawing. *Journal of IPSJ*, 40(3):1177–1187, 3 1999.

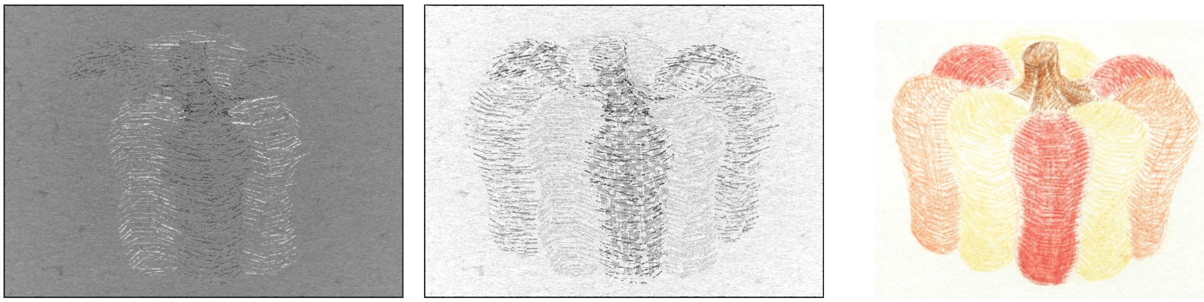

(a) Drawn on brown paper. (b) After watering. (c) Actual CPD after watering.

Figure 12. *Pumpkin* s after adding visual effects.

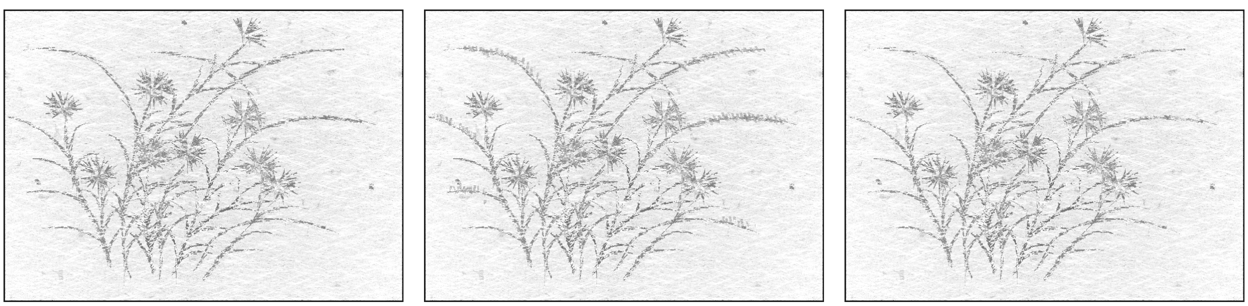

(a) CPD volume. (b) After watering. (c) Adding eraser effects.

(d) Colored pencil drawing. (e) After watering. (f) Adding eraser effects.

Figure 14. Colored pencil drawings on Japanese paper called "washi" and actual colored pencil drawings.